Quantum mechanical treatment of the F+D2→DF+D reaction

N. Abusalbi, C. L. Shoemaker, D. J. Kouri, J. Jellinek, and M. Baer

Citation: The Journal of Chemical Physics **80**, 3210 (1984); doi: 10.1063/1.447074
View online: http://dx.doi.org/10.1063/1.447074
View Table of Contents: http://scitation.aip.org/content/aip/journal/jcp/80/7?ver=pdfcov
Published by the AIP Publishing

Quantum mechanical treatment of the $F + D_2 \rightarrow DF + D$ reaction

N. Abusalbi,[a] C. L. Shoemaker,[a] and D. J. Kouri[a),b]
Department of Chemistry and Department of Physics, University of Houston—University Park, Houston, Texas 77004

J. Jellinek[c]
Department of Chemical Physics, Weizmann Institute of Sciences, Rehovot, Israel 76100

M. Baer
Applied Mathematics, Soreq Nuclear Research Center, Yavne, Israel 70600

(Received 1 July 1983; accepted 28 October 1983)

Reactive infinite order sudden (RIOS) approximation calculations for the $F + D_2 \rightarrow DF + D$ reaction using the Muckerman 5 potential are reported. Primitive γ-dependent state resolved reaction amplitudes and probabilities, γ-averaged probabilities, vibrational state resolved angular distributions, total integral cross sections, and vibrational branching ratios are presented. The results are compared against results of other methods and against similar RIOS results for the $F + H_2 \rightarrow HF + H$ reaction. The accuracy of the RIOS results is discussed and in addition, qualitative comparison with experimental vibrational state resolved angular distributions is made. We find that the RIOS $F + D_2$ results are similar to RIOS results for the $F + H_2$ system. Similarly, experimental results for these two systems are in qualitative agreement with one another. In the case of comparison of RIOS and experimental vibrational state resolved angular distributions, qualitative agreement is obtained for the $v_f = 3,2,1$ DF product states. However, the RIOS results for DF ($v_f = 4$) are strongly backward scattered while most recent experiments show strong forward peaking. Analogously, the RIOS results for HF ($v_f = 3$) are strongly backward scattered while the most recent experimental results show strong forward peaking. Detailed analysis of the RIOS results using Smith's lifetime matrix approach to characterizing resonances has been carried out. Clear evidence supporting the existence of resonances in the $F + D_2$ system is found. The implications of all these results for the potential surface are discussed.

I. INTRODUCTION

The development of nonpertubative quantal approximations for three dimensional reactive scattering is very important and is currently being pursued by several groups.[1–12] Of the available methods, one of the most widely applied has been the reactive infinite order sudden (RIOS) approximation.[4–7,10,12] This method has now been applied to the $H + H_2$, $F + H_2$, $D + H_2$, and $D + HCl$ reactions. In the case of $H + H_2$, qualitatively correct results were obtained for angular distributions and relatively good quantitative agreement was obtained for total reactive cross sections compared to exact close coupling (CC) results.[4,5,13] In the case of the $F + H_2$ system,[16] the l-av RIOS results for the total integral reactive cross sections agreed well with Muckerman's classical trajectory (CT) results.[14] Evidence suggested that the total integral reactive cross section is not subject to large quantum effects[6] and thus the RIOS appeared to give acceptable accuracy for such state summed quantities. The branching ratios for different product vibrational states appeared however to show large quantum effects,[6] in qualitative agreement with the j_z-conserving results of Redmon and Wyatt[3] (obtained with a somewhat different potential surface). Of particular interest were the angular distributions of the HF product molecules as a function of final vibrational state v_f. This is due to the fact that only for two systems ($F + H_2$ and $F + D_2$) is such state resolved data currently available.[15] Furthermore, the experiments show a fascinating behavior in which at the lowest energy, all HF products were backward scattered while at a slightly higher energy, all HF product molecules continued to be backward scattered except the $v_f = 2$ product, which was sideways scattered. (More recent studies suggest, however, that there is a significant forward peak in the $v_f = 3$ HF product.) This was tentatively interpreted in terms of a mechanism in which the well known $v_f = 2$ collinear resonance[16] for the $F + H_2$ system was shifted to higher orbital angular momentum as the energy was increased until ultimately, a shift to sideways scattering occurred.[15,3] The RIOS calculations using the Muckerman 5 potential[14] were in qualitative agreement with this shift from backwards to sideways scattering of the HF ($v_f = 2$) product but did not unambiguously indicate that a resonance mechanism was responsible.[6] There was evidence that resonance effects could be present but not necessarily

[a] Partial support of this research under National Science Foundation Grant CHE82-15317 is gratefully acknowledged.
[b] Acknowledgment is made to the donors of the Petroleum Research Fund, administered by the American Chemical Society, for partial support of this research.
[c] Chaim Weizmann Fellow. Present address: Department of Chemistry and The James Franck Institute, University of Chicago, Chicago, Illinois 60637.

 0021-9606/84/073210-13$02.10

that they were solely responsible for the shift in the angular pattern for the HF ($v_f = 2$) products. Other model calculations have recently been reported that also show sideways peaking of the $v_f = 2$ HF product.[17,18] In addition, they show backward scattering for the $v_f = 3$ HF product at both the low and higher energy. Of these, only the Bowman *et al.*[17] results included a sum over all final HF rotational states.

Classical trajectory (CT) calculations have been performed by Ron, Baer, and Pollak (RBP)[19(a)] for a single energy $E_{\text{tot}} = 0.5$ eV (which is somewhat higher than the experimental energies). The RBP study consisted of both forward and reverse CT calculations. The forward study showed only backwards scattering for all four final vibrational states, and in this sense confirmed the previous forward CT results obtained by Blais and Truhlar.[19(b)] In the case of the reverse CT calculations, a different picture was obtained. There are many accessible rotational states of the HF molecule which can be populated at the nominal experimental energies. Therefore, the reverse CT studies had to be done for a variety of rotational states. It was found that all rotational states for HF in the $v = 3$ state yielded backwards scattering, but several of the most probable rotational states for HF with $v = 2$ yielded sideways scattering. It was felt by RPB that these results point up a technical problem with the forward CT calculations having to do with boxing of the HF rotational-vibrational states. In the reverse CT calculations, one boxes on the final H_2 states and begins the calculation in a well defined HF rotational-vibrational state. Thus, RPB contend that the CT results taken as a whole cannot be considered to support the existence of quantum effects in the vibrational state selected angular distributions. Thus, in order to establish the presence of quantum effects such as resonances, one must carry out quantum calculations over a range of energies and analyze the results in order to see if a resonance complex is formed. An important point for the present discussion is the fact that the RIOS *does* qualitatively produce the sideways shift of the HF ($v_f = 2$) angular distribution observed experimentally for $F + H_2$ (and as a quantal method, it possesses the ability to describe both resonant effects such as occur in the collinear $F + H_2$ system as well as effects related to the quantization of the vibrational levels of the HF product).

In addition to the $F + H_2$ system, Sparks *et al.*[15,21] also performed measurements on the $F + D_2$ system. Collinear calculations for this system also show interesting resonance behavior, although the resonance appears to be significantly broader[22] than in the case of collinear $F + H_2$. The experimental results for this system showed pure backward scattering for DF (v_f) for all v_f at a relative kinetic energy of 2.34 kcal/mol while at 4.51 kcal/mol, the products are scattered progressively more forward. The results show the $v_f = 4$ DF product is more strongly forward peaked than backward at 4.51 kcal/mol, with the sequence $v_f = 3,2,1$ as one goes to larger scattering angle. Thus, the DF experimental results agree qualitatively with the newer HF experimental results which appear to show the $v_f = 3$ HF product with significant forward scattering, followed by the $v_f = 2$ and then the $v_f = 1$ HF products.

Recently, Ron, Pollak, and Baer[20] have performed a forward CT calculation also for the $F + D_2$ system at the two nominal experimental energies. Again, in contrast to the experimental results and the preliminary quantum RIOS results,[7] all the state-to-state differential cross sections were found to be scattered backward.

In the present paper, we present the detailed RIOS results for $F + D_2$ and compare them with various other results. In Sec. II, we present a brief summary of the RIOS equations and details of the calculation. In Sec. III, we describe the results obtained for various quantities. In Sec. IV, we discuss and compare our RIOS results with (a) the CT results for the total integral reactive cross section, (b) the previous RIOS results for $F + H_2$ and (c) the qualitative experimental results. Finally Sec. V contains a summary of our conclusions.

II. SUMMARY OF RIOS EQUATIONS AND CALCULATION DETAILS

The RIOS method employed is that discussed in an earlier series of papers.[4,6] In this method, fixed internal orientation reactive scattering (collinear-like) calculations are carried out yielding reactive S matrices $S^{n_\lambda}_{ln_\nu}(\gamma_\lambda)$, where n_γ is the vibrational state in arrangement $\gamma (= \lambda$ or $\nu)$, l is the IOS orbital angular momentum parameter,[23] γ_λ is the angle between the λ-arrangement diatom axis and the λ-arrangement center-of-mass system scattering vector. The Arthurs–Dalgarno[24] S matrices are obtained from the $S^{n_\lambda}_{ln_\nu}(\gamma_\lambda)$ according to

$$
\begin{aligned}
S^{\lambda n_\lambda j_\lambda l_\lambda}_{J\nu n_\nu j_\nu l_\nu} = i^{l_\lambda + l_\nu - 2l} \sum_{\Omega_\lambda \Omega_\nu} \frac{\sqrt{[l_\nu][l_\lambda]}}{[J]} \\
\times \langle l_\lambda 0 j_\lambda \Omega_\lambda | J \Omega_\lambda \rangle \langle l_\nu 0 j_\nu \Omega_\nu | J \Omega_\nu \rangle \\
\times 2\pi \int_0^\pi d\gamma_\lambda \sin\gamma_\lambda Y^*_{j_\nu \Omega_\nu}[\gamma_\nu(B,\gamma_\lambda),0] \\
\times d^J_{\Omega_\lambda \Omega_\nu}[\Delta(\gamma_\lambda,B)] Y_{j_\lambda \Omega_\lambda}(\gamma_\lambda,0) S^{n_\lambda}_{ln_\nu}(\gamma_\lambda),
\end{aligned}
\tag{1}
$$

where

$$
[K] = K(K+1), \tag{2}
$$

and Δ is defined as

$$
\Delta = \cos^{-1}(\hat{R}_\lambda \cdot \hat{R}_\nu). \tag{3}
$$

B is the matching surface parameter relating the λ and ν arrangements via

$$
r_\nu = B r_\lambda, \tag{4}
$$

and it is taken to be 1.4 for the present calculations. (This is the same value used in earlier $F + H_2$ studies.[6,25] Evidence there[25] indicated the results were not highly sensitive to the value of B.) The state-to-state differential scattering amplitude, in the helicity representation, is given by

$$
\begin{aligned}
f(\nu n_\nu j_\nu m_\nu | \lambda n_\lambda j_\lambda m_\lambda | \theta\phi) \\
= \frac{i^{j_\lambda - j_\nu + 1}}{2k_{j_\lambda}} \sum_J [J] d^J_{m_\lambda m_\nu}(\theta) S^{\lambda n_\lambda j_\lambda m_\lambda}_{J\nu n_\nu j_\nu m_\nu},
\end{aligned}
\tag{5}
$$

where

TABLE I. Integral reactive cross sections ($Å^2$) $F + D_2 \rightarrow DF + D$ $E_{tot} = 0.291$ eV.

Transition	$l_{initial}$	l_{av}	CT
0–0	0.5446 D − 04	0.9921 D − 04	0.0
0–1	0.7016 D − 02	0.1409 D − 01	0.0
0–2	0.2040 D + 00	0.4586 D + 00	0.494 D + 00
0–3	0.8843 D + 00	0.2060 D + 01	0.121 D + 01
0–4	0.2478 D − 01	0.5159 D − 01	0.467 D + 00
Total	0.1120 D + 01	0.2584 D + 01	0.217 D + 01

TABLE II. Integral reactive cross sections ($Å^2$) $F + D_2 \rightarrow DF + D$ $E_{tot} = 0.385$ eV.

Transition	$l_{initial}$	l_{av}	CT
0–0	0.3221 D − 03	0.6279 D − 03	0.0
0–1	0.1982 D − 01	0.3741 D − 01	0.195 D − 01
0–2	0.3741 D + 00	0.7910 D + 00	0.901 D + 00
0–3	0.1070 D + 01	0.2475 D + 01	0.209 D + 01
0–4	0.2652 D + 00	0.6627 D + 00	0.705 D + 00
Total	0.1729 D + 01	0.3967 D + 01	0.372 D + 01

$$S^{\lambda n_\lambda j_\lambda m_\lambda}_{J\nu n_\nu j_\nu m_\nu} = \sum_{l_\lambda l_\nu} i^{l_\lambda - l_\nu} \frac{\sqrt{[l_\lambda][l_\nu]}}{[J]} \times \langle l_\lambda 0 j_\lambda m_\lambda | J m_\lambda \rangle \langle l_\nu 0 j_\nu m_\nu | J m_\nu \rangle S^{\lambda n_\lambda j_\lambda l_\lambda}_{J\nu n_\nu j_\nu l_\nu}. \quad (6)$$

In most of the calculations reported herein, the CS-l parameter was taken to be the l-av choice. This means that in Eq. (1), for given l_λ, l_ν, the value of l is

$$l = (l_\lambda + l_\nu)/2. \quad (7)$$

The Muckerman 5 potential surface was used without modification.[14] The basis set convergence was such that unitarity was satisfied to better than 0.1% for almost every l value. The maximum deviation from unitarity (which occurred in two or three partial waves) was 1%. The calculations included a total of 18 vibrational states, and 30 partial waves were required at the low energy of 2.34 kcal/mol and 50 at the higher energy of 4.51 kcal/mol. The fixed γ_λ reactive probabilities were completely converged to zero by $\gamma_\lambda \geqslant 50°$ for the low energy and 60° for the higher energy.

III. RESULTS

A. Integral reactive cross sections

We now present the results obtained in these RIOS calculations for $F + D_2$. We begin with those for the vibrational state resolved reactive integral cross sections. These are given in Tables I and II for the two energies of interest. This quantity was calculated using both the l-av and l-initial versions[4,5] of the RIOS. In addition, we give the classical results of Ron, Pollak, and Baer[20] and also the results of the l-av RIOS calculation for $F + H_2$ in Table III for comparison. Finally, we show in Fig. 1 a comparison of the l-initial and l-av RIOS results for the total integral reactive cross section with various classical trajectory (CT) results.[14,20,26] As can be seen, there is excellent agreement between the l-av RIOS and the CT results.

B. Primitive results: γ-dependent probabilities

In Figs. 2 and 3 we give the reactive state-to-state probabilities as a function of γ for different l values. The results for $v_f = 1$ at $E_{tot} = 0.291$ and 0.385 eV are shown in Figs. 2(a) and 3(a), respectively, for $v_f = 2$ in Figs. 2(b) and 3(b), for $v_f = 3$ in Figs. 2(c) and 3(c) and $v_f = 4$ in Figs. 2(d) and 3(d). The main features are: (a) the probabilities for $v_f = 1,2,3$ are qualitatively different as a function of γ and l from those for $v_f = 4$. The probabilities for $v_f = 1,2,3$ tend to peak at angles away from the collinear while those for $v_f = 4$ tend to have their maximum at $\gamma = 0°$. Further, the qualitative features are essentially the same at both the low and higher energy and (b) any differences between the results at 0.291 and 0.385 eV total energy do not appear to be of an essential nature. The main changes are that all probabilities extend to larger γ values at the higher energy. The $v_f = 4$ results with $l = 0$ and $l = 5$ *do* show a slight maximum away from the $\gamma = 0$ angle but higher l's remain peaked at $\gamma = 0$.

Comparing the $F + D_2$ results with the corresponding $F + H_2$ results[6b] it is noted that qualitatively, the two sets of results are the same.

Next, in Fig. 4 we give some results for the energy dependence of the fixed γ probabilities for the $v_i = 0 \rightarrow v_f = 3$ and $v_i = 0 \rightarrow v_f = 4$ reactive transitions for the orbital angular momentum quantum numbers $l = 0$, 10, and 20. Results for $\gamma = 0°$, 15°, and 30° are shown. It is clear that as γ increases, the threshold for reaction goes up in energy. Similarly, as l increases, the threshold energy increases. Surprisingly, however, we find that initially as γ increases, the maximum value of the $P^l_{3,0}$ reaction probability increases. Again, the same effect is seen when l is increased (at least at lower γ angles). In the case of the $v_i = 0 \rightarrow v_f = 4$ reaction, however, increasing l causes a decrease in the maximum reaction probability, as does also increasing γ for fixed l.

In Figs. 5 and 6, we give Argand plots of the fixed γ reactive S-matrix elements for the $v_i = 0 \rightarrow v_f = 3$ reaction

TABLE III. Integral cross sections for the reaction $F + H_2(v_i = 0) \rightarrow HF(v_f = 0, 1, 2, 3, \Sigma v_f) + H$ (improved quantal l_{av}-IOSA results).

E_{tot} eV $\sigma(Å^2)$	0.310 $E_{tr} = 0.037\,208$	0.340 $E_{tr} = 0.067\,208$	0.360 $E_{tr} = 0.087\,208$	0.423 $E_{tr} = 0.150\,208$	0.500 $E_{tr} = 0.227\,208$
(0–0)	0.7698 D − 04	0.4679 D − 03	0.9475 D − 03	0.3808 D − 02	0.9881 D − 02
(0–1)	0.2498 D − 01	0.9106 D − 01	0.1460	0.3435	0.5769
(0–2)	0.8356	1.873	2.369	3.290	3.792
(0–3)	0.1912 D − 03	0.6722 D − 02	0.3246 D − 01	0.4380	1.131
σ total	0.8608	1.971	2.548	4.076	5.509

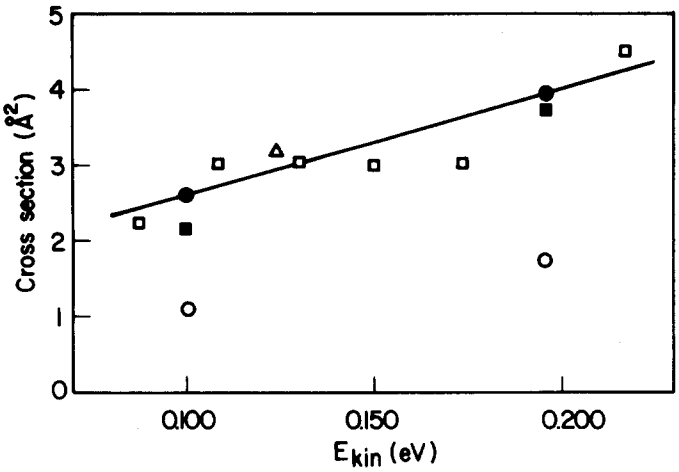

FIG. 1. Total reactive cross sections for $F + D_2 \rightarrow DF + D$: ○ l-initial RIOSA; ● l-average RIOSA; □ CT (Ref. 14); ■ CT (Ref. 20); △ CT (Ref. 26). The straight line goes through the two l-av RIOSA points.

process (we include results for l-0, 10, and 20). Results for $\gamma = 0°$ and $\gamma = 15°$ are shown. The characteristic feature of these results is the occurrence of a flattened portion of the Argand plot. Earlier collinear ($\gamma = 0°$) studies of $F + D_2$ with $l = 0$ showed this same behavior[22] and it was found in that case to signal the presence of a resonance in the presence of a strong nonresonant background. To examine this further, we carried out an eigenphase analysis of the $\gamma = 0°$, $l = 0$ S matrix with the results shown in Fig. 7. We find a characteristic "avoided crossing" behavior such as was discussed earlier by Kuppermann.[22] A more precise demonstration of the presence of resonances in the fixed-γ S matrices was carried out using the lifetime matrix analysis of Smith.[27] The results of these calculations are given in Figs. 8–13. The proper delay times for given γ and l values are presented as a function of energy and it is found that there is a significant delay indicating the occurrence of a resonance complex being formed in the $F + D_2$ system. When $\gamma = 0°$, it is found that the time delay experienced decreases (relatively slowly) as a function of orbital angular momentum. Similar behavior is also found for $\gamma \neq 0°$. Furthermore, the magnitude of the time delay also decreases as γ increases. These results show unequivocably that resonances are occurring over the range of γ and l values (even though the intensity of the resonance is varying). We also point out that the nonresonant time delays are all negative, which indicates that the duration of the reactive collision is shorter than the transit

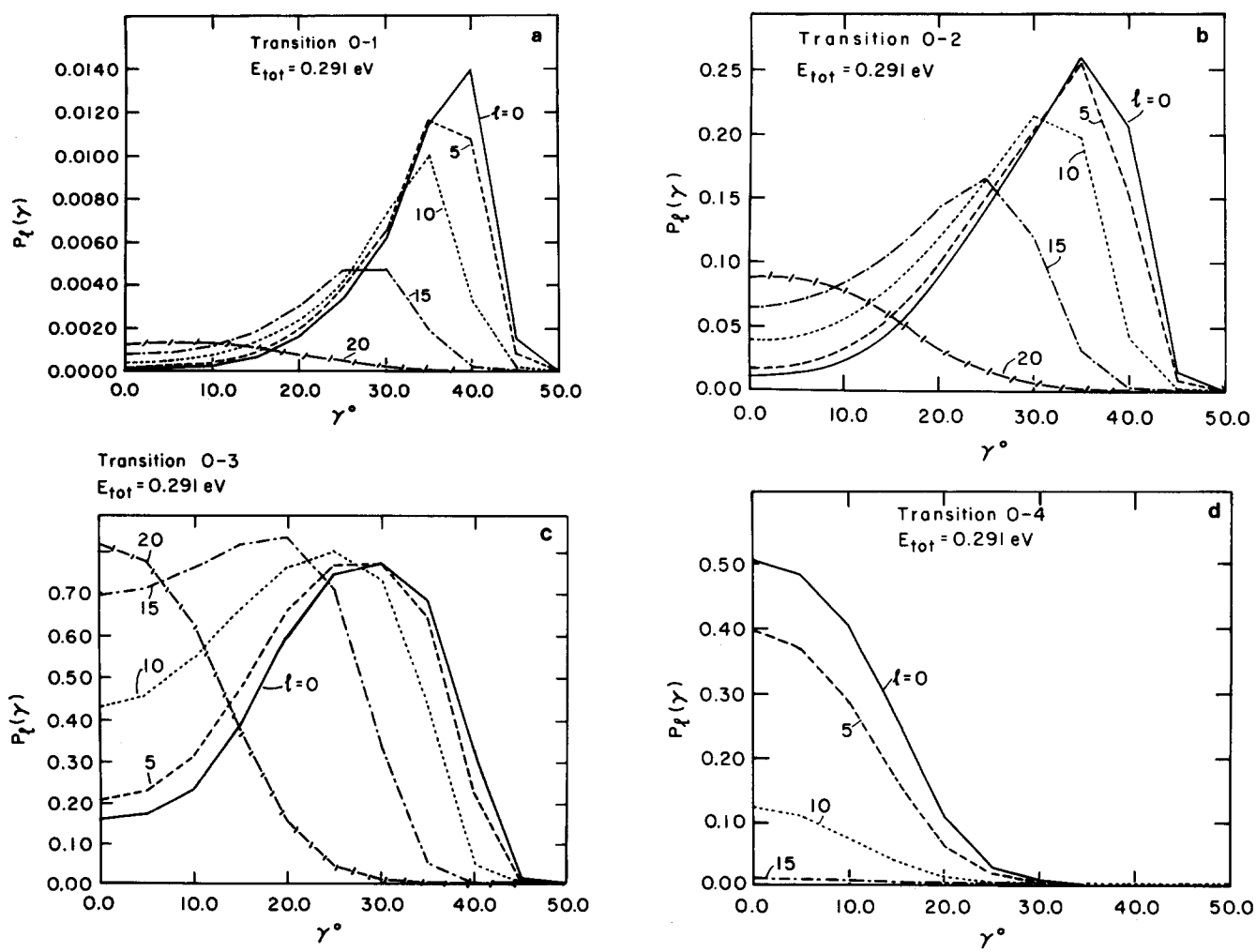

FIG. 2. Primitive reaction state-to-state probabilities $P(v = 0 \rightarrow v')$ as a function of γ_λ for different l values. The energy is $E_{tot} = 0.291$ (a) $P(v = 0 \rightarrow v' = 1)$; (b) $P(v = 0 \rightarrow v' = 2)$; (c) $P(v = 0 \rightarrow v' = 3)$; (d) $P(v = 0 \rightarrow v' = 4)$.

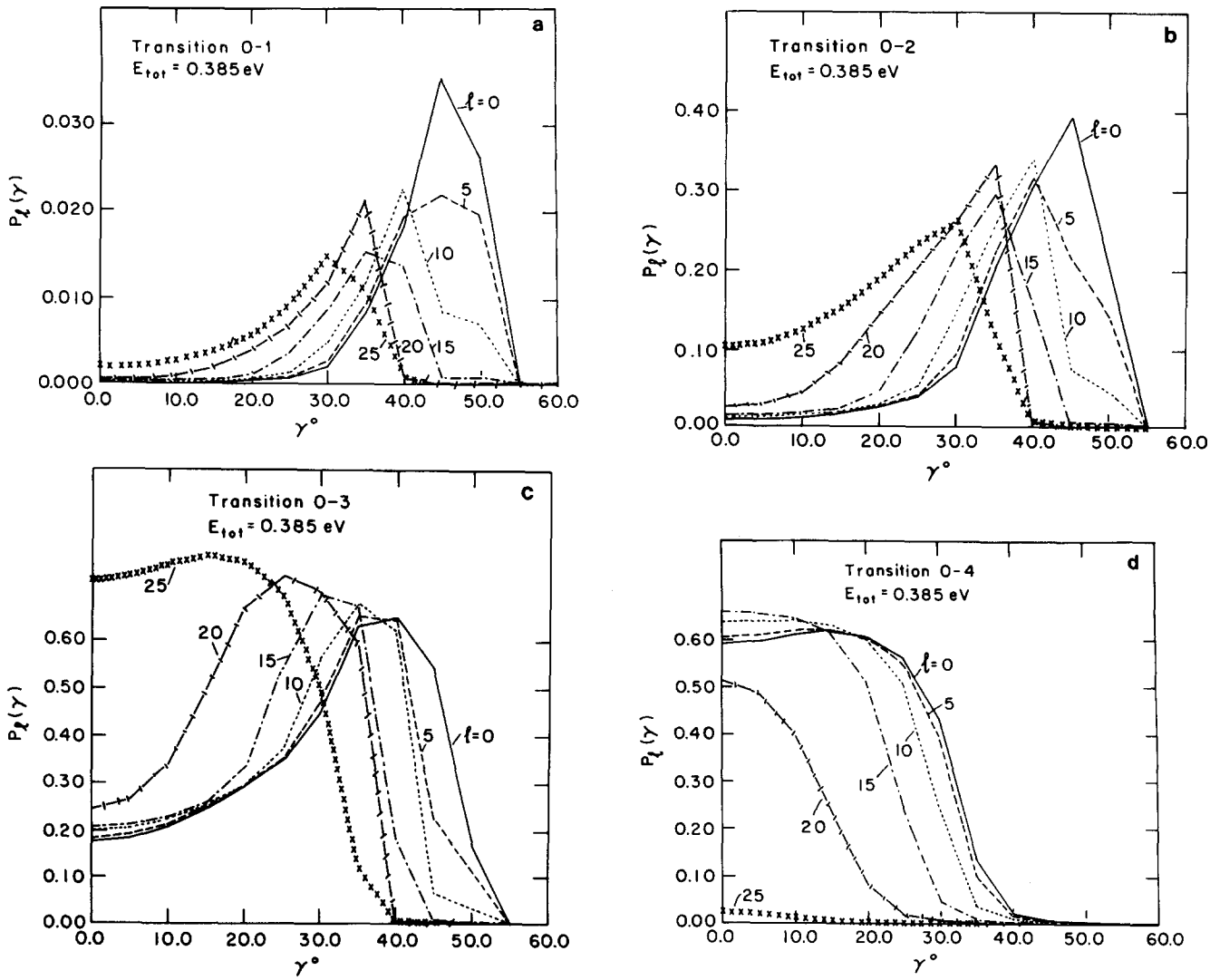

FIG. 3. Primitive reaction state-to-state probabilities $P(v=0 \rightarrow v')$ as a function of γ_λ for different l values. $E_{tot} = 0.385$ eV. (a) $P(v=0 \rightarrow v'=1)$; (b) $P(v=0 \rightarrow v'=2)$; (c) $P(v=0 \rightarrow v'=3)$; (d) $P(v=0 \rightarrow v'=4)$.

time that would occur if no interaction were present.

In Table IV, we give the actual maximum delay times for the $6(l,\gamma)$ cases considered and compare these times to the characteristic rotation and vibration times of the free D_2 molecule. It may be seen that the delay times typically permit the D_2 molecule to vibrate a few times but not to complete even a single rotation (of course, the D_2 molecule's motion would be perturbed by the presence of the F atom in the reaction zone so these comparisons are of a hypothetical nature). This is relevant from the standpoint of the accuracy of the sudden approximation for this collision system.

C. Angle averaged results

In Figs. 14 and 15 we present the results of vibrational resolved reactive probabilities, integrated over γ, as a function of l.[6] These curves are very similar to the curves obtained for the $F + H_2$ system.[6(b)] In particular, they should be compared with those with $E = 0.36$ and 0.5 eV, for which the $F + D_2$ initial kinetic energies are very close (for $F + D_2$, we have 0.0975 and 0.19 eV as the initial relative kinetic energies while for $F + H_2$, the corresponding values are 0.087 and 0.227 eV). Again, the qualitative correspondence between the $v_f = 1,2,3$ DF and $v_f = 1,2$ HF curves and between the $v_f = 4$ DF and $v_f = 3$ HF curves is evident. The DF curves for $v_f = 1,2,3$ extend to larger l values and have a more rectangular form while those for $v_f = 4$ have their maximum at $l = 0$.

D. State resolved angular distributions

In Figs. 16 and 17, we present the RIOS vibrational state resolved angular distributions. Each curve is scaled to equal one at $\theta = \pi$. We may summarize the results at 2.91 kcal/mol as follows: (a) the DF molecules are back scattered for $v_f = 1,2,3,4$; (b) the least backward peaked is $v_f = 3$ and the most is $v_f = 4$; and (c) interesting undulations are observed. The general features of the 4.51 kcal/mol results are: (a) the $v_f = 1,2,3$ DF molecules have all developed pronounced sideways peaks; (b) the order of the peaks (as the scattering angle is increased from zero toward π) is first $v_f = 3$, then $v_f = 2$ and finally $v_f = 1$; and (c) the $v_f = 4$ DF product continues to show very strong backward peaking and shows a pronounced minimum in the forward direction.

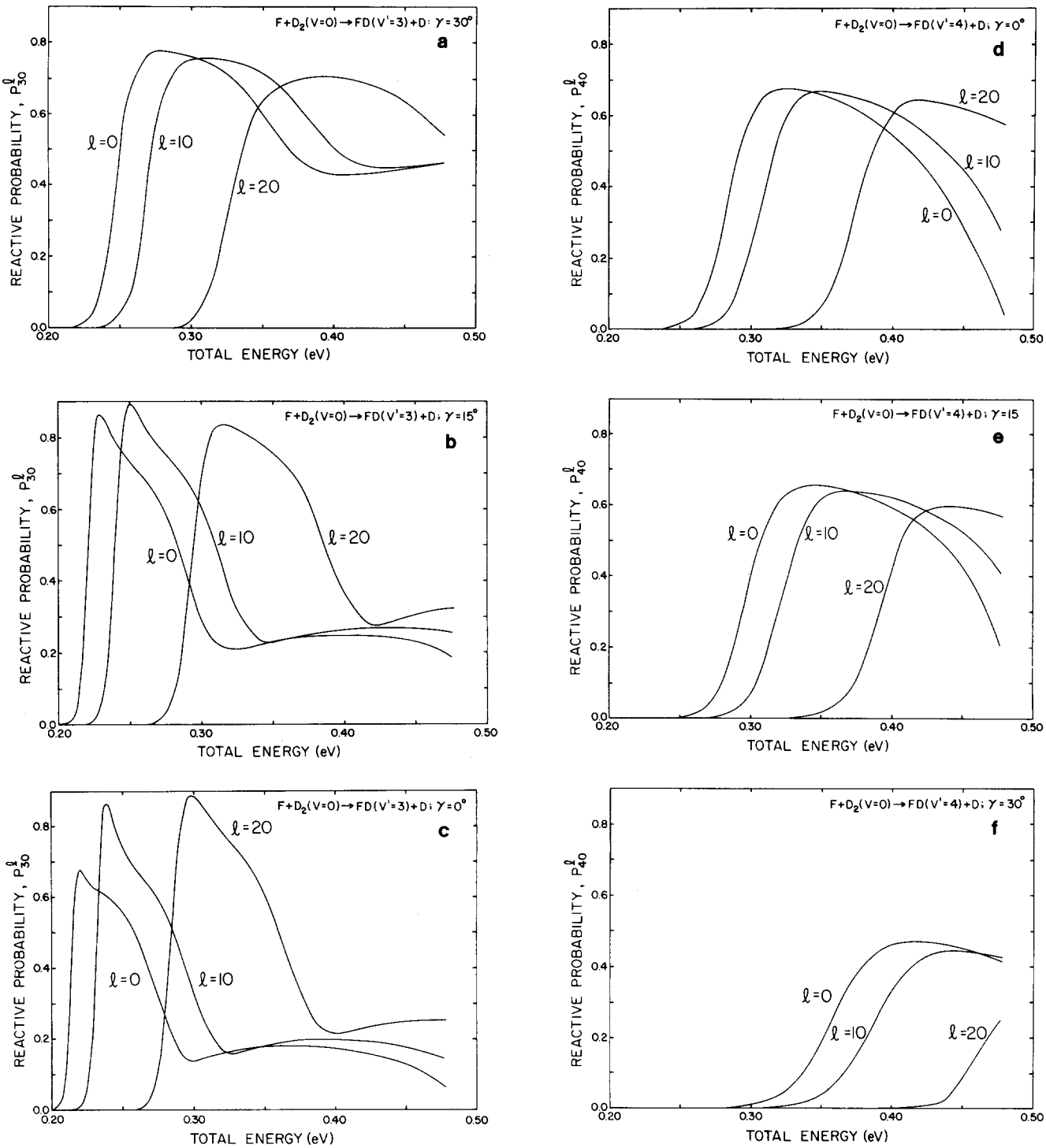

FIG. 4. Primitive reactive state-to-state probabilities $P(v=0 \rightarrow v')$ as a function of energy for different γ and l values. (a) $\gamma=0$; $v'=3$; (b) $\gamma=15$; $v'=3$; (c) $\gamma=30°$; $v'=3$; (d) $\gamma=0$; $v'=4$; (e) $\gamma=15$; $v'=4$; (f) $\gamma=30$; $v'=4$.

For purposes of comparison, we also show in Figs. 18 and 19 the analogous results for the $F+H_2$ system. It is immediately seen that the $v_f=3$ HF results are analogous to the $v_f=4$ DF results and similarly for the $v_f=2$, 1 HF and $v_f=3,2,1$ DF results. Note the oscillations in the HF results and also note that the $v_f=2,1$ HF results actually have a maximum not precisely at $\theta=\pi$ but rather slightly before π. The same behavior can be seen in the $v_f=3,2,1$ DF angular distributions.

The final quantities of interest are the branching ratios for scattering into various v_f states of the DF product. These are given in Table V and compared with the corresponding CT values.[20] We now turn to a detailed discussion of these results.

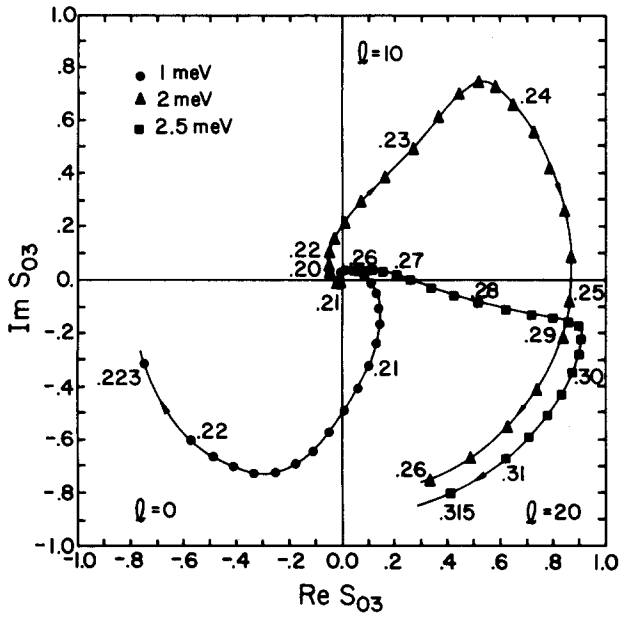

FIG. 5. Argand plot of the fixed-γ S matrix vs total energy for the process $F + D_2(v_i = 0) \rightarrow DF(v_f = 3) + D$ for various l values. $\gamma = 0°$.

IV. DISCUSSION

In the discussion we concentrate on several aspects of the computational results. First, we consider the accuracy of the RIOS results. Next we make a cross comparison of experimental and theoretical results for both the $F + D_2$ and $F + H_2$ systems. Third we consider the resonance effects and the tuning mechanism introduced in our earlier study of the $F + H_2$ system. We then consider the branching of the DF product among vibrational states. Finally, we consider the adequacy of the Muckerman 5 potential in light of the theoretical and experimental results for the $F + D_2$ and $F + H_2$ systems.

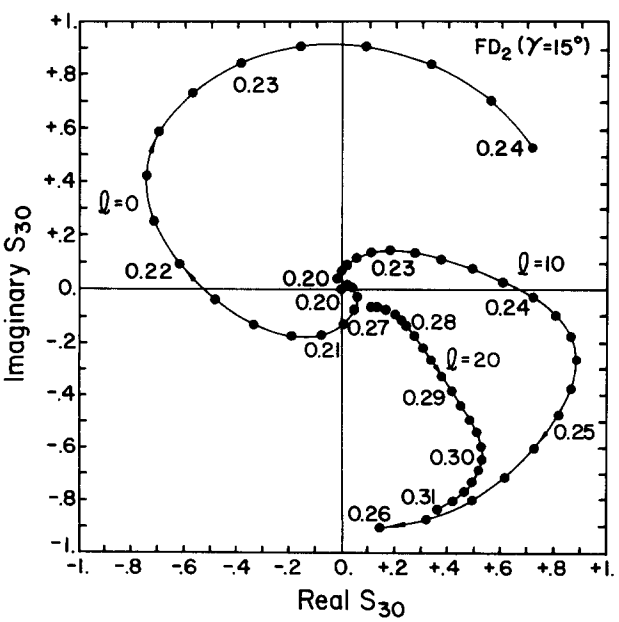

FIG. 6. Argand plot of the fixed-γ S matrix vs total energy for the process $F + D_2(v_i = 0) \rightarrow DF(v_f = 3) + D$ for various l values. $\gamma = 15°$.

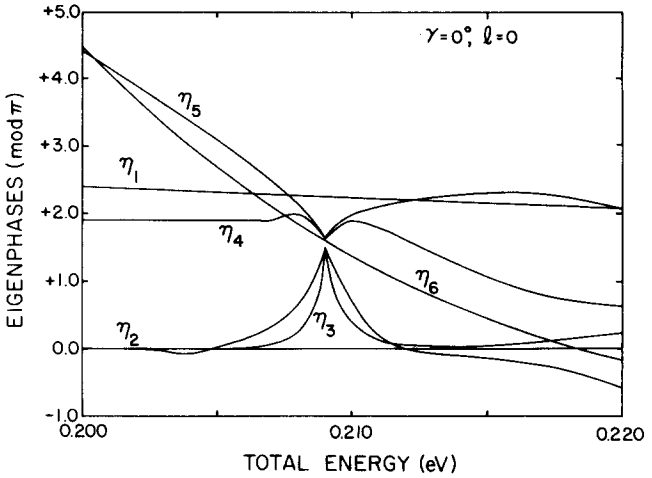

FIG. 7. Eigenphase shifts for $F + D_2$ collisions with $\gamma = 0°$, $l = 0$ plotted vs total energy.

A. Accuracy of the RIOS results

It is not an easy task to assess the quantitative accuracy of the RIOS method for the $F + D_2$ and $F + H_2$ systems because there does not exist exact quantum mechanical results for them. As a result, one is forced to compare either with results of other approximate methods or with experiment. Comparison with experiment is complicated by the fact that the effects due to the dynamical approximations and to the use of a semiempirical potential energy surface are difficult to disentangle. Thus, the best that one can do is to find quantities which can be reliably obtained by an independent approximate method for the same potential surface and

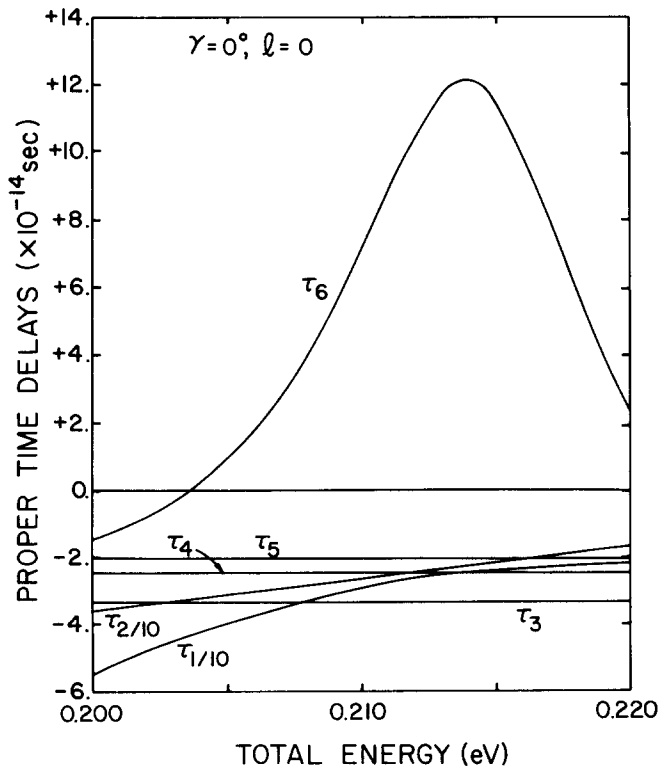

FIG. 8. Proper (eigen) delay times in units of 10^{-14} s for $\gamma = 0°$, $l = 0$ plotted vs total energy. τ_6 is dominated by the DF ($v_f = 3$) state.

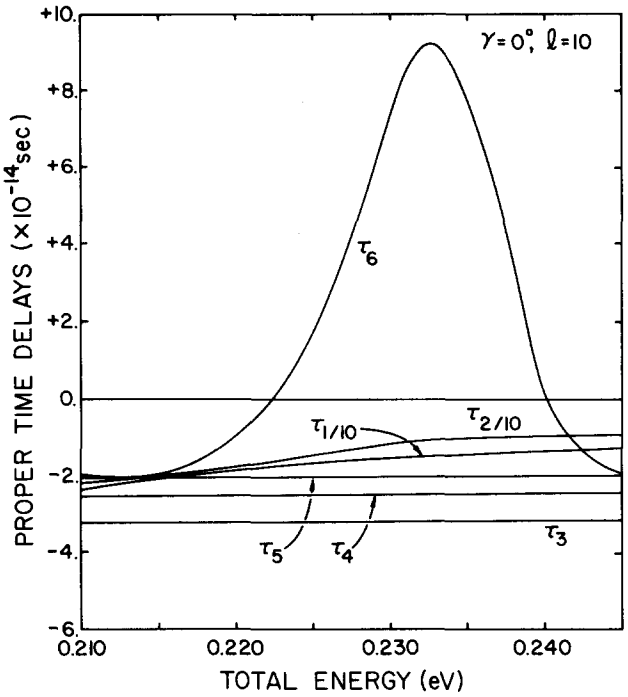

FIG. 9. Same as Fig. 8, except $\gamma = 0°$, $l = 10$.

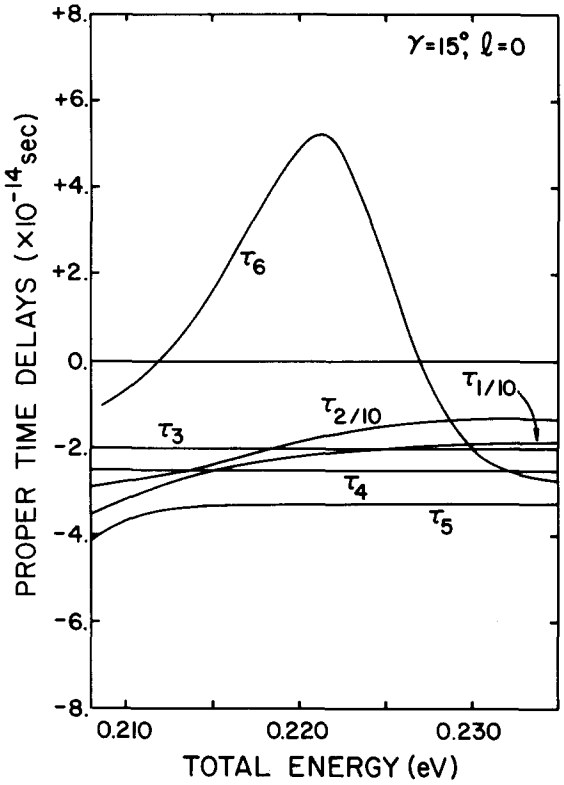

FIG. 11. Same as Fig. 8, except $\gamma = 15°$, $l = 0$.

proximate method for the same potential surface and compare results for these quantities. We believe that the CT method yields sufficiently reliable results for the total integral reactive cross section for the $F + D_2$ system, and have therefore chosen this is one of the quantities to use in assessing the accuracy of the RIOS method. Evidence that indicates that quantum effects are unimportant for the total reactive cross sections of the $F + H_2$ system includes the fact that classical and quantum l-initial labeled RIOS results for this quantity were in quantitative agreement.[25,6] The *only* difference between these two methods was the classical vs quantum aspect. In addition, the more sophisticated l-av RIOS results for $F + H_2$ were also in good agreement with exact CT results.[6] In the present case, consideration of Tables I and II, and of Fig. 1 shows that the l-av RIOS and exact CT results are in quantitative agreement for the $F + D_2$ system, so far as the total integral reactive cross section is concerned.

An interesting question regards the satisfaction of the sudden condition when one has a time delay due to a resonant collision. If the lifetime of the resonance complex is too long, then the sudden condition will certainly be violated. However, as was noted in Table IV, although the resonance

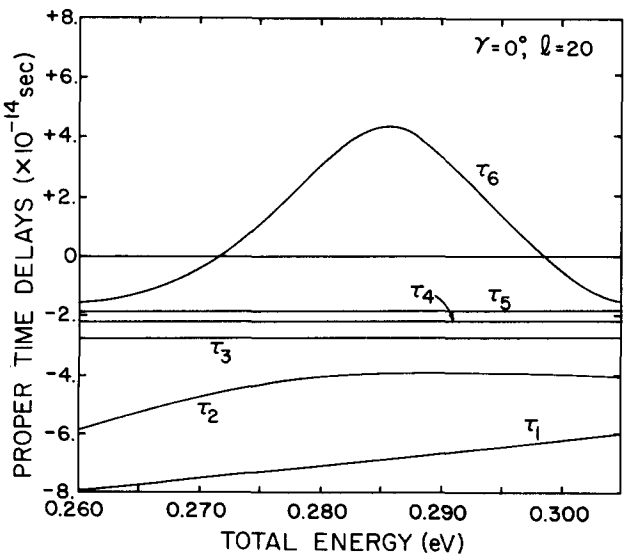

FIG. 10. Same as Fig. 8, except $\gamma = 0°$, $l = 20$.

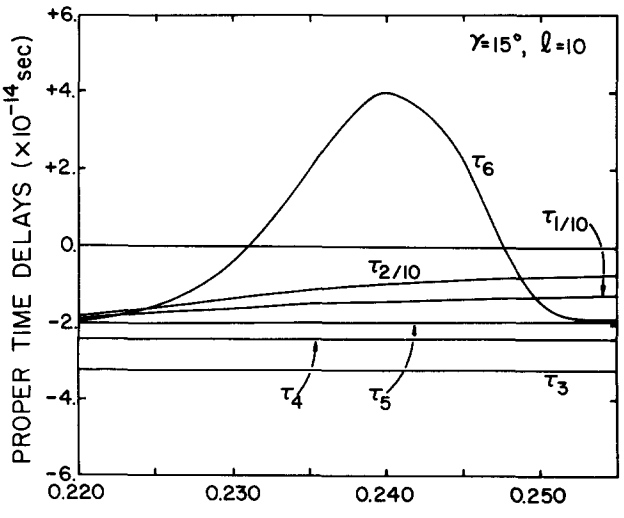

FIG. 12. Same as Fig. 8, except $\gamma = 15°$, $l = 10$.

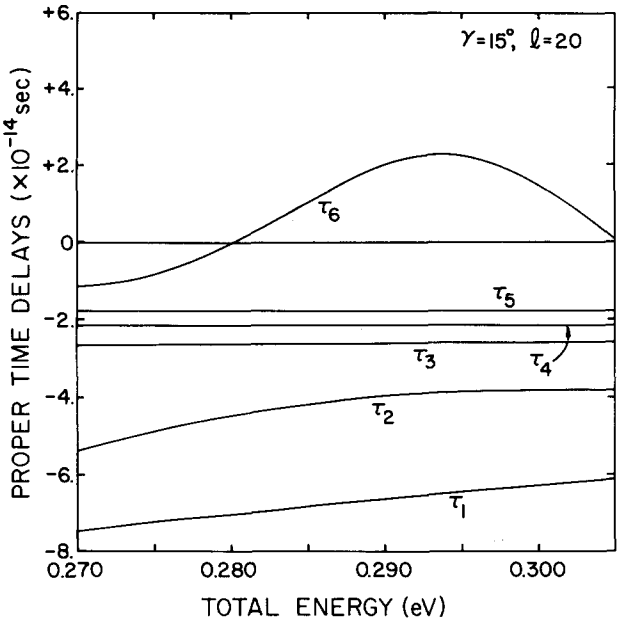

FIG. 13. Same as Fig. 8, except $\gamma = 15°$, $l = 20$.

complex lasts for a significant number of vibrations, the lifetime is still short compared to the characteristic rotation time of a free D_2 molecule. Thus, it will be even shorter compared to the rotation time of the DF product. Since the sudden approximation is being applied to molecular rotation (and *not* to vibration), we conclude that the presence of a resonance complex in this system does not lead to serious violation of the rotational sudden condition.

The question of accuracy of angular distributions is more difficult. Although we do not claim quantitative accuracy for these, we do believe their qualitative features are reliable. In the $H + H_2$ system [the only case where comparison of RIOS angular distributions with exact quantum close coupling (CC) is feasible] this was in fact the case.[28] This system is much more unfavorable to the RIOS than is the $F + D_2$ since one has an H_2 molecule in every arrangement. We, therefore, believe that the present results are likely to be at least qualitatively correct.

There is next the question of the accuracy of branching ratios into various vibrational quantum levels. In the earlier work on $H + H_2$, it was found that the branching for the reaction with H_2 intially in the $v = 1$ state agreed well with other quantal sudden approximations as well as with limited close coupling results.[4] The CT results for this do not agree well with quantum results. In the case of the $F + H_2$ system, again CT vs quantal sudden results disagree but the quantum results obtained by the l-initial and l-av versions of the RIOS agree very well with one another. This is also the case for $F + D_2$. In addition, the RIOS branching ratios agree qualitatively with those obtained by Redmon and Wyatt[3] using a j_z-conserving method (they, however, used a modified version of the Muckerman 5 potential surface). We believe that the branching ratios predicted by the RIOS method are more reliable than those obtained with CT methods and that these quantities manifest strong quantum effects.

Another important question regarding accuracy of the RIOS has to do with the effects of the bending angle for the triatomic system. This bending is completely neglected in a collinear model and also in the simplest rotating linear model.[18] This causes the threshold for reaction in such models to occur at too low an energy since energy no longer gets "trapped" in this degree of freedom. Its effect in collinear based approximations and in the rotating linear model has been approximately taken into account by subtracting the zero point energy for the bending *as a function of the reaction coordinate*.[18,29] Since this lowers the amount of relative kinetic energy available, it leads to a higher threshold energy for the reaction. Since it varies with reaction coordinate, it acts like an additional potential energy. In the RIOS method, we do not do such a subtraction of the bending zero point energy from the available kinetic energy. However, the RIOS method *does* include an effect of the dependence of the reaction on the bending variable in an alternative approximate fashion. It enters because the RIOS method involves an average of reaction amplitudes calculated with the full potential at all possible values of γ, and the potential energy increases as γ moves away from the collinear value $\gamma = 0$. This causes the fixed-γ amplitudes to die out as γ increases. *The physical amplitude, as can be seen in Eq. (1), is an average over γ so that again the threshold for reaction will be increased over that which would be obtained in the collinear case.* This effect is very clearly seen in Fig. 4. Thus, the RIOS automatically includes at least part of the effect of the variation of reactivity due to bending. Of course, it does not include it in precisely the same way as is done in the rotating collinear model. Both techniques are approximate average methods for including the effect of the fact that energy gets

TABLE IV. Proper time delays for $F + D_2 \rightarrow FD + D$.

	$\gamma=0°, l=0$	$\gamma=0°, l=10$	$\gamma=0°, l=20$	$\gamma=15°, l=0$	$\gamma=15°, l=10$	$\gamma=15°, l=20$
τ_{delay} [1]	1.4×10^{-13}	1.15×10^{-13}	5.76×10^{-14}	7.2×10^{-14}	6.0×10^{-14}	3.4×10^{-14}
$\frac{\tau_{delay}}{\tau_0^{vib}}$ [2]	13.0	10.7	5.4	6.6	5.5	3.1
$\frac{\tau_{delay}}{\tau_0^{rot}}$ [3]	0.13	0.10	0.055	0.07	0.05	0.03

[1]Units are in s.
[2]This is the number of times a free D_2 molecule in the $v = j = 0$ state will vibrate during the collision.
[3]This is the number of times a free D_2 molecule will rotate during the collision.

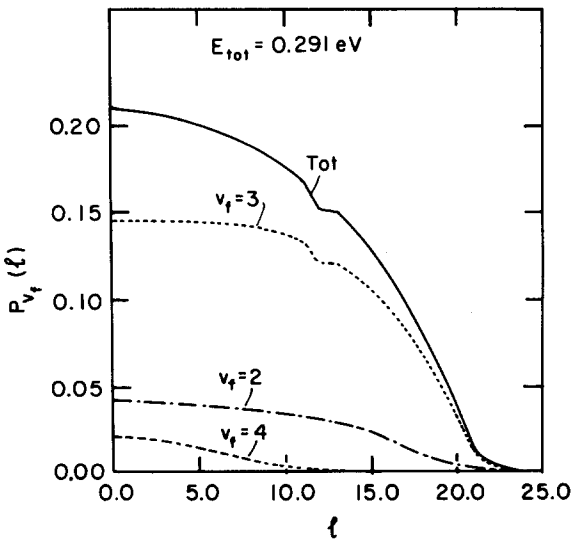

FIG. 14. Angle averaged state-to-state F + D_2→DF + D reaction probabilities as a function of l for $E_{tot} = 0.291$ eV.

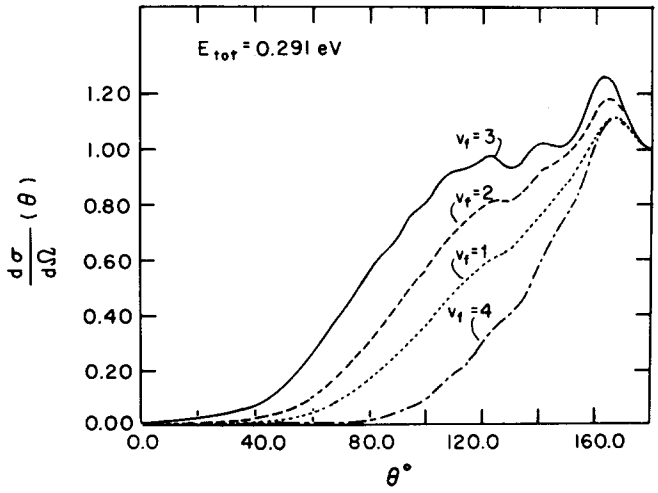

FIG. 16. Vibrational state resolved differential cross sections for F + D_2→DF + D for $E_{tot} = 0.291$ eV. All cross sections are normalized to one at $\theta = 180°$.

absorbed by the bending degree of freedom.

In summary, we believe there is reasonable evidence indicating that (a) the RIOS result for the total integral reactive cross section is quantitatively accurate for the F + D_2 system; (b) the vibrational state resolved angular distributions are qualitatively reliable; (c) the branching ratios for scattering into various final vibrational states of FD are also qualitatively reliable; and (d) the qualitative increase in the threshold for reaction due to energy in the bending degree of freedom is included approximately.

B. Comparison of the F + H_2 results, F + D_2 results, and experiment

One of the most striking features of the F + D_2 results is the extremely strong qualitative resemblance they bear to the F + H_2 results. In Figs. 2 and 3 we presented the l-dependent probabilities for various l values. It would appear that the $v_f = 1,2,3$ DF results are in correspondence with the $v_f = 1,2$ HF results, while the highest accessible DF product, $v_f = 4$, corresponds with the highest accessible HF product, $v_f = 3$.[6(b)] Thus, the major factor appears to be the smaller zero point energy of the DF molecule compared to that for HF but the basic dynamics on the Muckerman 5 potential are essentially the same. Of course, there are differences in the magnitudes of cross sections obtained for the two systems at either a given total energy (due to the fact that this results in different relative collision energy because of the different vibrational energy) or at a given initial relative kinetic energy. The latter leads to different results for several reasons. First, at the same relative kinetic energy, the translational velocity of the F relative to the center of mass of the D_2 will not be the same as that for F relative to the center of mass of the H_2 due to the different reduced masses for the relative motion in the two cases. Secondly, in the final ar-

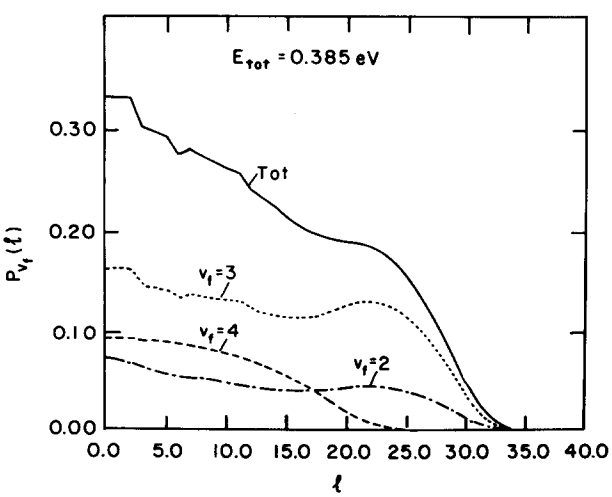

FIG. 15. Same as Fig. 14, except $E_{tot} = 0.385$ eV.

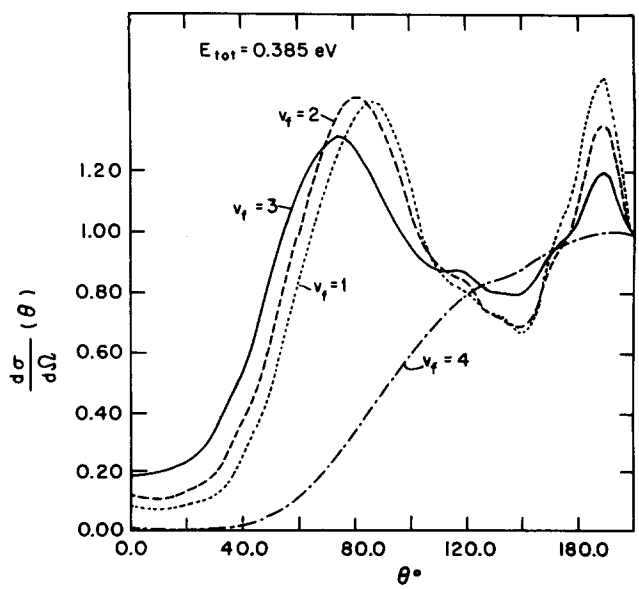

FIG. 17. Same as Fig. 16, except $E_{tot} = 0.385$ eV.

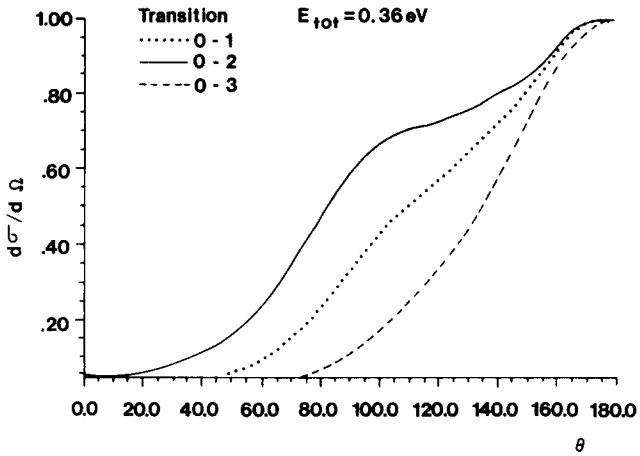

FIG. 18. Vibrational state resolved differential cross sections for $F + H_2 \rightarrow HF + H$ for $E_{tot} = 0.36$ eV. All cross sections are normalized to one at $\theta = 180°$.

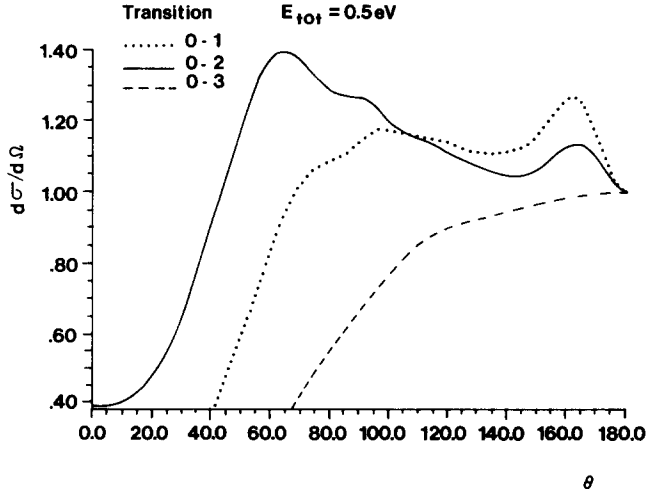

FIG. 19. Same as Fig. 18, except $E_{tot} = 0.5$ eV.

rangement, the relative kinetic energy of the exiting atom will also be different for the $F + D_2$ and $F + H_2$ systems again due to the differences in projectile reduced masses and vibrational energies of the product molecules. However, in spite of these differences, there is a good correspondence between the behavior of the $v_f = 4$ DF and $v_f = 3$ HF products, of the $v_f = 3$ DF and $v_f = 2$ HF products and of the $v_f = 2$ DF and $v_f = 1$ HF products.

Next, we note in Figs. 16–19 the strong resemblances between the angular distributions for the DF and HF products, with again the $v_f = 4$ DF and $v_f = 3$ HF behaving similarly and the $v_f = 3,2,1$ DF and $v_f = 2,1$ HF products behaving similarly. In the case of experimental results, it also would appear that the $F + D_2$ and $F + H_2$ systems behave qualitatively the same. Thus in $F + H_2$ the most recent results indicate that the $v_f = 3$ is forward peaked while in $F + D_2$, it is the $v_f = 4$ which is forward peaked. Then as one moves away from the forward direction, the $v_f = 2$ HF and $v_f = 3$ DF are next in order of increasing scattering angle, followed by the $v_f = 1$ HF and $v_f = 2$ DF.[15,21] Thus, the latest experimental data shows a similar correspondence between the v_f state of HF with the $v_f + 1$ state of DF. The present theoretical results agree qualitatively with the experimental results so far as the $v_f = 3,2,1$, DF product and $v_f = 2,1$ HF product angular distributions but disagree with experiment for the $v_f = 4$ DF and $v_f = 3$ HF products. *However, even in this instance, the theoretical and experimental results agree that these products behave similarly.* Regarding the backward angular distribution of the $v_f = 4$ DF product (and analogously the $v_f = 3$ HF product), there seems to be little chance, in our opinion, that the Muckerman 5 surface can result in behavior other than this. If the experimental findings are indeed correct, then we believe this is clear evidence that the Muckerman 5 surface is not capable of fully describing the vibrational state resolved angular distributions.

The final feature of the angular distributions which is of interest is the occurrence of oscillations. In our earlier study of $F + H_2$,[6] it was speculated that these oscillations might be due to interference between resonant and nonresonant contributions to the scattering amplitude. An alternate explanation is that the scattering into different final rotational states of the product molecule may peak at different scattering angles. (The angular distributions shown in Figs. 16–19 are summed over all final rotational states.) Again we see qualitative agreement between the $F + D_2$ and $F + H_2$ results in the occurrence of such oscillations.

C. Resonances in the $F + D_2$ system

The lifetime matrix analysis of the present $F + D_2$ results settles the question of whether resonances are occurring in the RIOS treatment of this system. In addition, the qualitative similarity between our $F + D_2$ and $F + H_2$ fixed-γ, fixed-l reaction probabilities strongly suggests that the same type resonances occur in the $F + H_2$ system. Indeed, in the $F + H_2$ work,[6] we proposed a "resonance tuning" mech-

TABLE V. Vibrational state branching ratios for the $F + D_2 \rightarrow FD + D$ reaction.

	$E_{tot} = 0.291$ eV ($E_{kin} = 0.098$ eV)			$E_{tot} = 0.385$ eV ($E_{kin} = 0.191$ eV)		
	l_{av}	$l_{initial}$	CT[a]	l_{av}	l_{av}	CT
$\lambda(1, 3)$[b]	6.84×10^{-3}	7.93×10^{-3}	0.0	1.51×10^{-2}	1.85×10^{-2}	0.01
$\lambda(2, 3)$	0.223	0.231	0.41	0.32	0.35	0.43
$\lambda(4, 3)$	2.50×10^{-2}	2.80×10^{-2}	0.39	0.27	0.25	0.34

[a] See Ref. 20.

[b] $\lambda(v, 3)$ is defined as $\sigma(v_i = 0, j_i = 0 \rightarrow v, \Sigma_{jf})/\sigma(v_i = 0, j_i = 0 \rightarrow 3, \Sigma_{jf})$.

anism to explain the shift from backward to sideways peaking of the $v_f = 2$ product. This resonance tuning mechanism consisted of the proposal that the collinear $\gamma = 0, l = 0$ resonance did not disappear quickly as γ and/or l increased but rather shifted to higher energy. In addition, the resonance was conjectured to broaden slowly as γ or l increased until eventually it did disappear. As a consequence of such a mechanism, one expects to observe a shift from backward scattering at low energy (since here it is the $\gamma = 0, l = 0$ or low γ, l values which are in resonance and they lead to backward scattering) to sideways scattering at higher energy for all product states involved in the resonance (which as γ, l increase, shifts to higher energy). This resonance tuning is very clearly manifested in the results shown in Figs. 4–13. We see, e.g., the shift to higher energy of the threshold (and the resonance occurs in the threshold region). In addition, as l is increased, the threshold energy increases. The resonance continues to occur as γ and/or l increase, but at ever higher energies. (However, the resonance does get broader.) As a result, it is at higher energies that the larger l values resonate and these correspond to the impact parameters that would result in a sideways shift of the reactive products. The resonance does not appear to influence the $v_f = 4$ DF product. As a consequence (for the energy range studied) the $v_f = 4$ DF product is predicted to be backward scattered. Of course, the most recent experimental results show the $v_f = 4$ DF product as being scattered forward. This would appear to indicate that if a resonance mechanism is indeed involved, it must affect not only the $v_f = 3$ DF product but also $v_f = 4$.

D. Branching ratios

The branching ratios in Table V also show a great similarity to the RIOS results for the branching ratio in FH_2. In particular, we find that essentially the same results are found regardless of whether one uses the l-av or l-initial versions of the RIOS. In addition, the predominant product is the $v_f = 3$ DF molecule at both the low and higher collision energy. At the higher energy, which corresponds to a initial kinetic energy of about 4.5 kcal, we also note that the $v_f = 2$ and 4 products are about equally populated.

In Table V are also given the corresponding CT branching ratios as obtained in the RPB study.[20] The main feature to be noted is the difference in the energy dependence of these ratios in the two approaches. The RIOS branching ratios are strongly energy dependent while the CT ones exhibit a weak energy dependence. In this respect we note that the RIOS and CT vibrational state-to-state distributions for the higher energy overlap (see Table II). The largest difference occurs for $v_f = 3$ where the deviation is about 20%. The experiments (which measure thermal rate constants rather than cross sections) done at 297[30] and 300 K[31] both show a similar magnitude for λ (2,3) and λ (4,3) but one shows λ (4,3) as larger than λ (2,3).[31] The detailed magnitudes of the experimental branching ratios λ (2,3) and λ (4,3) are larger than the RIOS and CT results.

E. Adequacy of the potential surface

We now turn to discuss evidence which we believe indicates that the Muckerman 5 potential surface possesses too steep a dependence on the bending angle γ. The types of results we examine are: (1) *ab inito* studies of the potential surface; (2) total rate constants for $F + H_2$ reaction compared to experiment; (3) vibrational state distribution of the HF products; and (4) experimental forward scattered angular distributions of the DF ($v_f = 4$) and HF ($v_f = 3$) product molecules compared to backward scattering for the theoretical results. The most detailed *ab initio* surface calculation for the $F + H_2$ system is that of Bender *et al.*[32] They find a surface whose dependence on bending angle γ is weaker than the Muckerman 5 surface. Unfortunately, the exothermicity of the surface is too low thereby making the surface unsuitable for carrying out RIOS calculations. However, we believe that such a weaker γ dependence will result in a significantly larger total reaction cross section. This is of importance in light of the fact that to date, all calculations of the total reaction rate constant for the $F + H_2$ reaction yield results substantially smaller than *any* available experimental results.[6,14] A weaker γ dependence should result in increased reaction probabilities for the noncollinear attacks. In addition, the quantal results for $F + H_2$ yield too low branching ratio λ (3,2) and for $F + D_2$ too low branching ratio λ (4,3). This is due to the rapid quenching of the reaction into the highest open vibrational state as γ deviates from zero due to these becoming locally closed channels when γ is too large. Again, the weaker γ dependence should result in increased reaction into the highest accessible product vibrational state. Finally, and of greatest interest, is the question of the experimental observation of forward scattering of the $v_f = 4$ DF product in $F + D_2$ and $v_f = 3$ HF product in $F + H_2$.[15] A weaker γ dependence of the potential should result in the $v_f = 4$ DF state being less dominated by the collinear configuration of the system. This in turn should permit the angular distribution of the DF ($v_f = 4$) product in the $F + D_2$ system to develop a significant nonbackward scattering component. A similar result should be seen for the HF ($v_f = 2$) product in the $F + H_2$ reaction system.

V. SUMMARY

In this paper, we have presented state resolved cross sections obtained by the RIOS method for the $F + D_2 \rightarrow DF + D$ reaction. The results show that this system behaves in a manner completely analogous to the $F + H_2 \rightarrow HF + H$ reaction. On the basis of our results using Smith's lifetime matrix analysis, it appears that both reactions have important effects due to resonances. Evidence has been presented indicating that the RIOS results are of sufficient accuracy to enable them to be used in analysing these two reactive systems. In fact, the total integral cross sections obtained for the $F + D_2$ reaction are believed to be quantitative, while the state resolved angular distributions are more likely to be semiquantitatie. Comparison of the state resolved angular distributions for $F + D_2$ with experimental results shows qualitative agreement for the $v_f = 3,2,1$ DF and $v_f = 2,1$ HF product molecules but *not* for the $v_f = 4$ DF and $v_f = 3$ HF products. However, experiment and theory *do* appear to agree that the $F + D_2$ and $F + H_2$ systems behave in a qualitatively completely analogous fashion. The qualitative disagreement between experiment and theory for

the $v_f = 4$ DF and $v_f = 3$ HF product angular distributions, the smaller rates compared to experimental results and the vibrational state branching ratios are believed to signal short comings in the Muckerman 5 potential surface. In particular, it is felt that these disagreements are due to the Muckerman 5 surface having too steep a dependence on the bending angle γ. In conclusion, we believe the RIOS method has predictive capability and can be used to study reactions for which experiments have not yet been carried out, in order to search, e.g., for interesting quantum effects in chemical reactions. In addition, the method can be used to analyze experimental results in order to gain important information concerning intermolecular interactions.

[1]See, for example the reviews by M. Baer, Adv. Chem. Phys. **49**, 191 (1982), and R. E. Wyatt, in *Atom–Molecule Collision Theory: A Guide for the Experimentalist*, edited by R. B. Bernstein (Plenum, New York, 1979), pp. 447–503.

[2]A. B. Elkowitz and R. E. Wyatt, Mol. Phys. **31**, 189 (1976).

[3]M. J. Redmon and R. E. Wyatt, Int. J. Quantum Chem. **11**, 343 (1977).

[4]V. Khare, D. J. Kouri, and M. Baer, J. Chem. Phys. **71**, 1188 (1979); M. Baer, V. Khare, and D. J. Kouri, Chem. Phys. Lett. **68**, 378 (1979); M. Baer, H. Mayne, V. Khare, and D. J. Kouri *ibid.* **72**, 269 (1980); J. Jellinek, M. Baer, V. Khare, and D. J. Kouri, *idib*, **75**, 460 (1980); V. Khare, D. J. Kouri, J. Jellinek, and M. Baer, in *Potential Energy Surfaces and Dynamics Calculations*, edited by D. G. Truhlar (Plenum, New York, 1981), pp. 475–493.

[5]J. M. Bowman and K. T. Lee, J. Chem. Phys. **68**, 3940 (1978); Chem. Phys. Lett. **64**, 29 (1979); J. Chem. Phys. **72**, 5071 (1980).

[6](a) J. Jellinek, M. Baer, and D. J. Kouri, Phys. Rev. Lett. **47**, 1588 (1981); (b) M. Baer, J. Jellinek, and D. J. Kouri, J. Chem. Phys. **78**, 2962 (1983); and (c) M. Baer, D. J. Kouri, and J. Jellinek (to be published).

[7]C. L. Shoemaker, D. J. Kouri, J. Jellinek, and M. Baer, Chem. Phys. Lett. **94**, 359 (1983).

[8]G. D. Barg and G. Drolshagen, Chem. Phys. **47**, 209 (1980).

[9]D. C. Clary, Mol. Phys. **44**, 1067, 1083 (1981).

[10]D. C. Clary and G. Drolshagen, J. Chem. Phys. **76**, 5027 (1982).

[11]R. B. Walker and E. F. Hayes, J. Phys. Chem. (in press).

[12]J. Jellinek and D. J. Kouri, in *Theory of Chemical Reaction Dynamics*, edited by M. Baer (CRC, Boca Raton, 1983); J. Jellinek, Ph.D. dissertation, Dept. of Chemical Physics, Weizmann Institute of Science, Rehovot, Israel.

[13]G. C. Schatz and A. Kuppermann, J. Chem. Phys. **65**, 4624, 4642, 4668 (1976).

[14]J. T. Muckerman, in *Theoretical Chemistry: Advances and Perspectives*, edited by H. Eyring and D. H. Henderson (Academic, New York, 1981), Vol. 6A.

[15]R. K. Sparks, C. C. Hayden, D. Shobatake, D. M. Neumark, and Y. T. Lee, in *Horizons in Chemistry*, edited by K. Fukui and B. Pullman (Reidel, New York, 1980); and Y. T. Lee (private communication).

[16]G. C. Schatz, J. M. Bowman, and A. Kuppermann, J. Chem. Phys. **56**, 1024 (1973); **63**, 674 (1975).

[17]J. M. Bowman, K.-T. Lee and G. -Z. Ju, Chem. Phys. Lett. **86**, 384 (1982).

[18]R. B. Walker and E. F. Hayes (to be published).

[19](a) S. Ron, M. Baer, and E. Pollak, J. Chem. Phys. **78**, 4414 (1983); (b) N. C. Blais and D. G. Truhlar, *ibid.* **76**, 4490 (1982).

[20]S. Ron, E. Pollak, and M. Baer, J. Chem. Phys. **79**, 5204 (1983).

[21]R. K. Sparks. K. Shobatake, and Y. T. Lee (private communication).

[22]A. Kuppermann, in *Potential Energy Surfaces and Dynamics Calculations*, edited by D. G. Truhlar (Plenum, New York, 1981).

[23]The question of the CS orbital angular momentum parameter is discussed extensively in P. McGuire and D. J. Kouri, J. Chem. Phys. **60**, 2488 (1974); R. T. Pack, *ibid.* **60**, 633 (1974); D. Secrest, *ibid.* **62**, 710 (1975); Y. Shimoni and D. J. Kouri, *ibid.* **65**, 3372, 3958 (1976); **66**, 675, 2841 (1977); D. G. Truhlar, R. E. Poling, and M. A. Brandt, *ibid.* **64**, 826 (1976); G. A. Parker and R. T. Pack, *ibid.* **66**, 2850 (1977); D. J. Kouri, and Y. Shimoni, *ibid.* **67**, 86 (1977); R. Goldflam and D. J. Kouri, *ibid.* **66**, 542 (1977); V. Khare, *ibid.* **67**, 2897 (1977); L. Monchick, *ibid.* **67**, 4626 (1977); D. J. Kouri, R. Goldflam and Y. Shimoni, *ibid.* **67**, 4534 (1977); D. E. Fitz, Chem, Phys. **24**, 133 (1977); V. Khare, D. J. Kouri, and R. T. Pack. J. Chem. Phys. **69**, 4419 (1978); D. E. Fitz, Chem. Phys. Lett. **55**, 202 (1978); R. Schinke and P. McGuire, Chem. Phys. **28**, 129 (1978); L. Monchick and D. J. Kouri, J. Chem. Phys. **69**, 3262 (1978); D. A. Coombe and R. F. Snider, *ibid.* **71**, 4284 (1979); S. Stolte and J. Reuss, in *Atom–Molecule Collision Theory: A Guide for the Experimentalist*, edited by R. B. Bernstein (Plenum, New York, 1979); D. J. Kouri, *ibid.*; V. Khare, D. J. Kouri, and D. K. Hoffman, J. Chem. Phys. **74**, 2275 (1981); V. Khare, D. E. Fitz, and D. J. Kouri, *ibid.* **73**, 2802, 4148 (1980); V. Khare and D. J. Kouri, Chem. Phys. Lett. **80**, 262 (1981); V. Khare, D. J. Kouri, and D. K. Hoffman, J. Chem. Phys. **74**, 2656 (1981).

[24]A. M. Arthurs and A. Dalgarno, Proc. R. Soc. London Ser. A **256**, 540 (1960).

[25]J. Jellinek and M. Baer, Chem. Phys. Lett. **82**, 162 (1981), and J. Chem. Phys. **78**, 4494 (1983).

[26]D. F. Feng, E. R. Grant, and J. W. Root, J. Chem. Phys. **64**, 3450 (1976).

[27]F. T. Smith, Phys. Rev. **118**, 349 (1960).

[28]D. J. Kouri, V. Khare, and M. Baer, J. Chem. Phys. **75**, 1179 (1981).

[29]J. M. Bowman, G. -Z. Ju, and K. T. Lee, J. Chem. Phys. **86**, 2232 (1982).

[30]M. J. Berry, J. Chem. Phys. **59**, 6229 (1973).

[31]D. S. Perry and J. C. Polanyi, Chem. Phys. **12**, 419 (1976).

[32]C. F. Bender, P. K. Pearson, S. V. O'Neil, and H. F. Schaefer, J. Chem. Phys. **56**, 4626 (1972).